

We are IntechOpen, the world's leading publisher of Open Access books Built by scientists, for scientists

6,900

Open access books available

186,000

International authors and editors

200M

Downloads

Our authors are among the

154

Countries delivered to

TOP 1%

most cited scientists

12.2%

Contributors from top 500 universities



WEB OF SCIENCE™

Selection of our books indexed in the Book Citation Index
in Web of Science™ Core Collection (BKCI)

Interested in publishing with us?
Contact book.department@intechopen.com

Numbers displayed above are based on latest data collected.
For more information visit www.intechopen.com



The Stability of a Three-State Unfolding Protein

Yang BinSheng

Institute of Molecular Science, Key Laboratory of Chemical Biology and Molecular Engineering of Ministry of Education, Shanxi University, Taiyuan

1. Introduction

The mechanism by which proteins fold to their unique native conformations from an initially disorganized form is one of the fundamental problems in molecular biology. In the study of proteins fold or refold standard Gibbs free energy, $\Delta G^0(\text{H}_2\text{O})$ is the single most important parameter for quantitating-protein stability and comparing stabilities of closely related proteins. Nearly all theoretical and experimental aspects of protein folding relate in some way to unfolding free energy changes, and much of the current work involving comparisons of mutant proteins is highly dependent on accurate evaluation of unfolding free energy measurements [1].

The history of evaluation of the quantity known as standard Gibbs free energy spans more than four decades, and at least three procedures involving strong solvent denaturation have been used in evaluation of this quantity. The three procedures are known as the transfer model of Tanford, the denaturant binding model, and the linear extrapolation method. Of the three methods employed in evaluation of $\Delta G^0(\text{H}_2\text{O})$ the so-called linear extrapolation method appears to enjoy the greatest acceptance. The virtue of the linear extrapolation method over the other two methods resides in the perception that it is more reliable since it gives $\Delta G^0(\text{H}_2\text{O})$ values that appear to be independent of whether urea or guanidinium hydrochloride is used as denaturant [2].

The linear extrapolation method is the most frequently used method of determining protein unfolding free energy changes induced by urea or guanidine hydrochloride (GdnHCl). It is based upon the premise that unfolding free energy changes are linearly dependent on denaturant concentration and that extrapolation to zero denaturant concentration gives $\Delta G^0(\text{H}_2\text{O})$, the unfolding free energy change in the absence of denaturant. When only the native and unfolded forms of protein are present in significant concentrations at equilibrium, $F \xrightleftharpoons{K} U$, the unfolded process corresponds to one transition, i.e. two-state model. The $\Delta G^0(\text{H}_2\text{O})$ can be obtained from $\Delta G = \Delta G^0(\text{H}_2\text{O}) + m[D]$, where m reflects the sensitivity of the transition to denaturant concentration $[D]$ by using the linear extrapolation method [3].

When the native, partially unfolded (stable intermediate) and unfolded forms of protein are present in significant concentrations at equilibrium, $F \xrightleftharpoons{K_{FI}} I \xrightleftharpoons{K_{IU}} U$, the unfolded process corresponds to two transitions, i.e. three-state model. Moreover, the $\Delta G_{\text{total}}^0(\text{H}_2\text{O})$ is

considered to be the sum of $\Delta G_{Fi}^0(\text{H}_2\text{O})$ and $\Delta G_{U_i}^0(\text{H}_2\text{O})$ [4-8]. By comparing the two-state and a three-state unfolding processes of proteins, the order of the unfolding free energy was always inconsistent with the order of stability observed. This raises the question about the accuracy of the evaluated unfolding free energy values of three-state models. In this chapter, the linear extrapolation method was considered as a standard method in the two-state unfolding model and particular attention is paid to the $\Delta G_{\text{total}}^0(\text{H}_2\text{O})$ terms of the three-state unfolding model.

2. Assumptions

1. The protein unfolding process is determined by the structural element, E_i . E_i can change from a native state, $E_i(F)$ to a denatured, unfolded state $E_i(U)$, in two-state model. S_F^i , S_U^i , are the measurable signal of the folded and unfolded states for E_i , respectively, which were assumed to not vary with denaturant concentration to minimize the number of parameters. The equilibrium between $E_i(F)$ and $E_i(U)$ is described in eq (1).

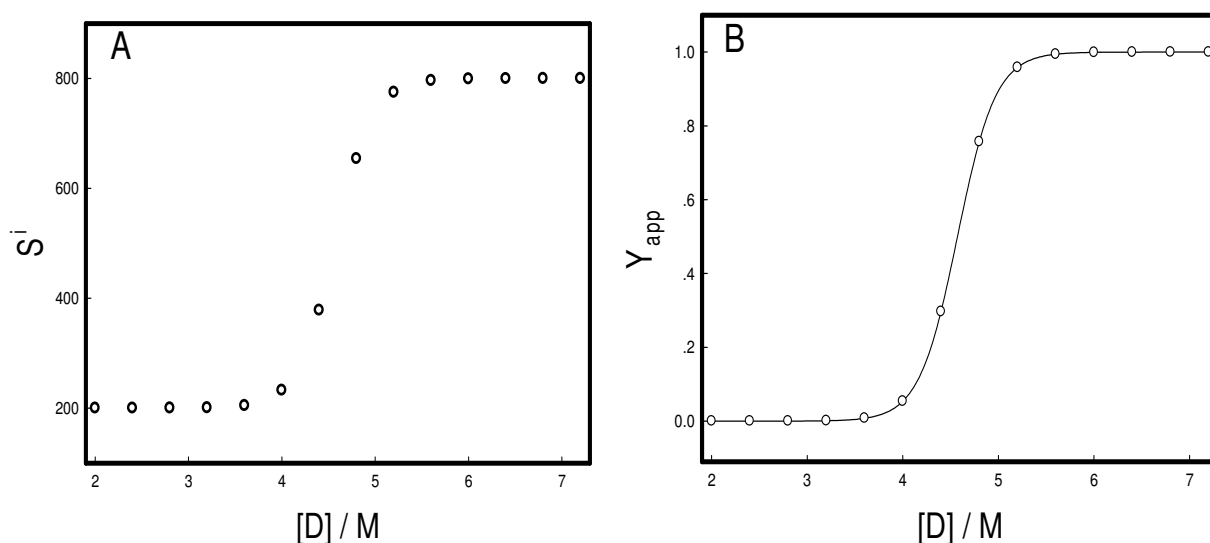


Fig. 1. The variation of S_i (A) and Y_{app}^i (B) of structural element, E_i , with the denaturant concentration. The observed data were fitted based on eq (3)

Figure 1A shows that the observed signals of the various experimental techniques (optical rotation, viscosity, UV-Vis absorption, fluorescence, circular dichroism, dynamic light scattering, nuclear magnetic resonance, etc) for structural element, E_i vary with the denaturant concentrations. At low denaturant concentrations (from $[D] = 2.0$ to $[D] = 3.0$) the measured signals are constant and can be considered as S_F^i , the signal of folded state. At high denaturant concentrations (from $[D] = 6.5$ to $[D] = 7.5$) the measured signals are constant, too, and can be considered as S_U^i , the signal of unfolded state. The unfolding curve of E_i , which is the plot of apparent fraction of unfolded structural element, Y_{app}^i against the denaturant concentrations, can be prepared as Figure 1B by using eq (2).

$$Y_{app}^i = \frac{S_o^i - S_F^i}{S_U^i - S_F^i} \quad (2)$$

where S_o^i is the observed signal at the given denaturant concentration

According to the linear extrapolation method the unfolding curve of E_i can be fitted based on eq (3).

$$Y_{app}^i = \frac{\exp(-\Delta G_i/RT)}{1 + \exp(-\Delta G_i/RT)} \quad (3)$$

where ΔG_i is the difference in free energy between the folded and the unfolded states of E_i at the given concentration of denaturant, R is the gas constant, and T is the absolute temperature. The equilibrium constant of unfolding transition is described in eq (4).

$$K_i = \frac{S_o^i - S_F^i}{S_U^i - S_o^i} \quad (4)$$

The free energy difference, ΔG_i can be evaluated following eq (5)

$$\Delta G_i = -RT \ln K_i = \Delta G_i^0(\text{H}_2\text{O}) + m_i[D] \quad (5)$$

$\Delta G_i^0(\text{H}_2\text{O})$ is the single most important parameter for quantitating structural element, E_i stability and comparing stabilities of closely related structural element, E_i . m_i is a measure of the dependence of ΔG_i on denaturant concentration.

From Figure 1B the plot of ΔG_i against the concentration of denaturant is shown in Figure 2. $\Delta G_i^0(\text{H}_2\text{O})$ and m_i can be obtained from Figure 2. They are $56.70 \text{ kJ mole}^{-1}$ and $-12.41 \text{ kJ mole}^{-1} \cdot \text{M}^{-1}$, respectively.

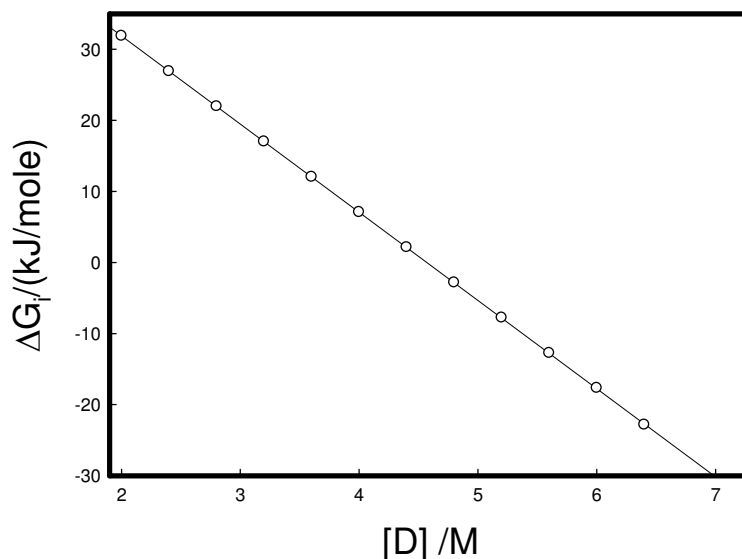


Fig. 2. The plot of ΔG_i against the concentration of denaturant at 25°C

When Y_{app}^i is 0.5 or the native and unfolded forms of structural element, E_i are 50%, respectively, the equilibrium constant of unfolding transition, K_i is 1. From eq (5) eq (6) can be obtained.

$$\Delta G_i^0(\text{H}_2\text{O}) = -m_i[D]_{1/2} \quad (6)$$

where $[D]_{1/2}$ is the midpoint concentration of denaturant required for unfolding of structural element. It means that we can use either m_i and $[D]_{1/2}$ as two parameters or $\Delta G_i^0(\text{H}_2\text{O})$ as single parameter to quantitate the structural element stability and compare the stabilities of closely related structural element. Only one $[D]_{1/2}$ or m_i is not enough to account for the stability of structural element, E_i .

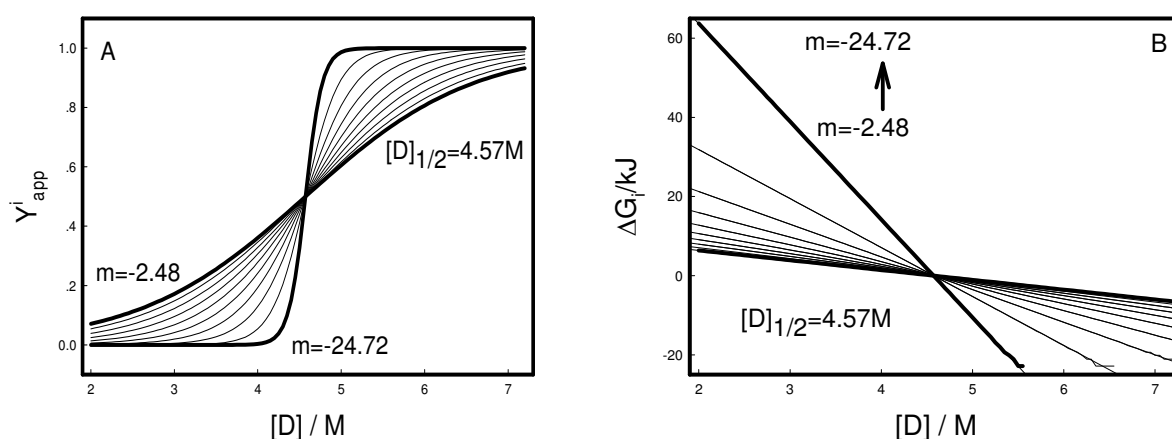


Fig. 3. The plots of Y_{app}^i (A) and ΔG_i (B) against the concentration of denaturant at 25°C

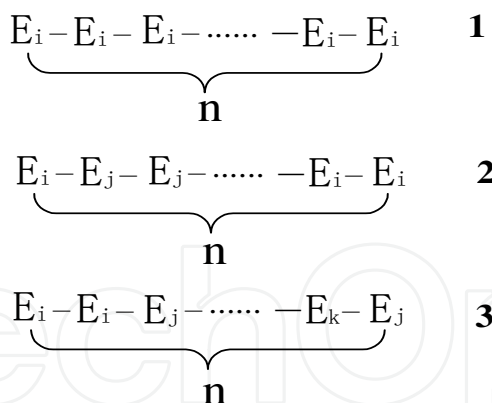
At $[D]_{1/2} = 4.57\text{M}$ the variations of Y_{app}^i and ΔG_i with the concentration of denaturant are shown in Figure 3. At constant m_i the unfolding curves corresponding to different $[D]_{1/2}$ are only shifts of a unfolding curve.

ΔG_i is a function of m_i and $[D]_{1/2}$, and can be written as $\Delta G_i(m_i, [D]_{1/2})$. Therefore, Y_{app}^i can also be written as $Y_{app}^i(m_i, [D]_{1/2})$.

2. Protein is consisted of structural elements connected by chemical bonds that there is no contribution to measured signal. When protein contains two kinds of structural elements, E_i and E_j , the three-state unfolding behavior may be observed. The observed three-state unfolding curve Y_{app} is composed of curves (Y_{app}^i) and (Y_{app}^j) mixed at a certain molar fraction.

If the number of structural elements is n , the protein can be express as scheme 1. Typical 1 of protein is consisted of same structural elements and typical 2 and 3 of proteins are consisted of different structural elements.

It is known that the unfolding of structural element, E_i obeys two-state model. The stability can be expressed as $\Delta G_i(m_i, [D]_{1/2})$ and the unfolding process can be described by $Y_{app}^i(m_i, [D]_{1/2})$. If m_i is $-24.72 \text{ kJ} \cdot \text{M}^{-1} \cdot \text{mole}^{-1}$ and $[D]_{1/2}^1$ is 2.57 M we can obtain $Y_{app}^1(-24.72 \text{ kJ} \cdot \text{M}^{-1} \cdot \text{mole}^{-1}, 2.57\text{M})$ from eq(3) and eq(5). Similarly, we can obtain $Y_{app}^2(-24.72 \text{ kJ} \cdot \text{M}^{-1} \cdot \text{mole}^{-1}, 6.57\text{M})$. There is a protein, in which the structural element, E_1 appears for n times. The measured unfolding data (\circ) of the protein are presented in Figure 4A.



Scheme 1. The proteins consisted of structural elements

Denaturant-induced unfolding of the protein is found to be a two-state process, just as that of the structural element, E_1 .

There is a protein, in which the structural element, E_1 appears for n_1 times and E_2 does for n_2 times. The sum of n_1 and n_2 is n . The measured unfolding data (\circ) of the protein are presented in Figure 4B. Denaturant-induced unfolding of the protein is found to be a two-step process with accumulation of an intermediate state at around 3.5~5.5 M denaturant concentration. Therefore, denaturant-induced denaturation may be considered as a three-state transition and the mechanism for unfolding of the protein may be represented as:



where F , I and U are the folding, intermediate and unfolding states of the protein, respectively. The first transition which corresponded to the transformation of F state to the I state started at around at 1.5 M denaturant concentration and completed at 3.5 M denaturant with a midpoint occurring at 2.57 M denaturant. In fact the transition corresponds to the unfolding of E_1 in the protein.

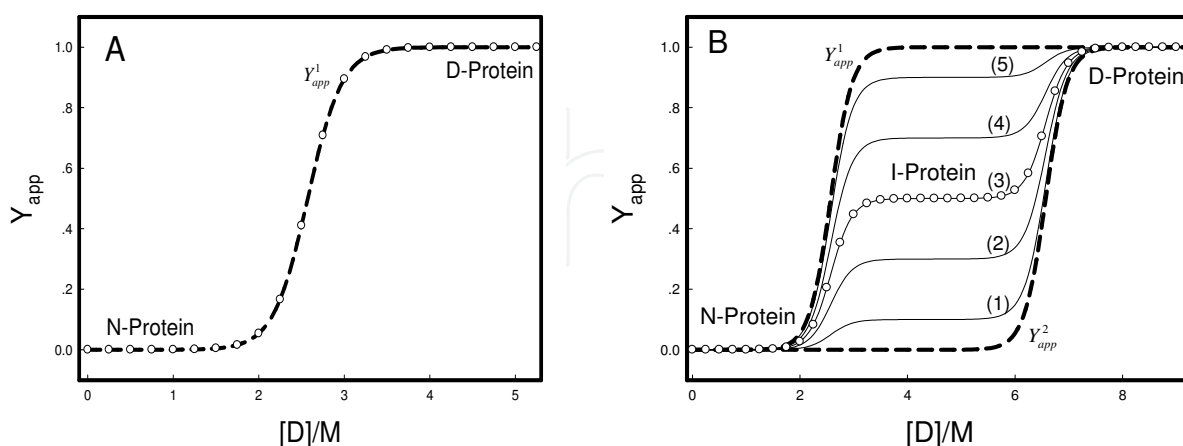


Fig. 4. The measured apparent fraction of unfolded proteins (\circ) at different denaturant concentrations. A: The protein consisted of same structural elements (E_1). B: a protein consisted of different structural elements (E_1 and E_2). Y_{app}^1 and Y_{app}^2 are the unfolding curves of E_1 and E_2 , respectively. Based on eq(8) curves (1)~(5) are obtained from f_1 as 0.1, 0.3, 0.5, 0.7, and 0.9, respectively.

The second transition, which corresponded to the unfolding of the I state, started at around 5.5 M denaturant concentration and finally sloped off to the U state at 7.7 M denaturant with a midpoint occurring at 5.57 M denaturant. The transition corresponds to the unfolding of E_2 in the protein. The intermediate state of the protein is a partial unfolding state, in which E_1 exists in completely unfolding form and E_2 does in completely folding form. The three-state unfolding process can be considered to be composed of two sequential two-state unfolding processes. Then the measured unfolding data (\circ) of the protein in Figure 4B can be fitted by using eq(8).

$$Y_{app} = f_1 \bullet Y_{app}^1 + f_2 \bullet Y_{app}^2 \quad (8)$$

where f_1 and f_2 are molar fractions of structural elements E_1 and E_2 in the protein.

$$f_1 = \frac{n_1}{n} \quad f_2 = \frac{n_2}{n} \quad n = n_1 + n_2 \quad (9)$$

From eq(8) it is known that f_1 or f_2 , Y_{app}^1 and Y_{app}^2 are the important factors to determine the three-state unfolding curve of protein. When f_2 is zero, the protein is consisted of structural elements, E_1 , which appear n time in the protein. The three-state unfolding curve changes into two-state unfolding curve, Y_{app}^1 . When f_1 is zero, the protein is consisted of structural elements, E_2 , which appear n time in the protein. The three-state unfolding curve changes into two-state unfolding curve, Y_{app}^2 .

Y_{app} has the scale as f_1 and f_2 . It can be seen that the measured stable intermediate state of the protein appears at $Y_{app} = 0.5$ from Figure 4B. So we could determine the f_1 or f_2 value to be 0.5.

Protein is consisted of structural elements, $E_1, E_2, E_3, \dots, E_{n-1}$, which appears $n_1, n_2, n_3, \dots, n_{n-1}$ times in the protein. The unfolding curves corresponding to $E_1, E_2, E_3, \dots, E_{n-1}$ are $Y_{app}^1, Y_{app}^2, Y_{app}^3, \dots$, and Y_{app}^{n-1} , respectively, and $m_i \neq m_j$, $[D]_{1/2}^i \neq [D]_{1/2}^j$ (i and j change from 1 to $n-1$). The unfolding curve of the protein would be a n -state unfolding curve and can be fitted using eq(10).

$$\begin{aligned} Y_{app} &= f_1 \bullet Y_{app}^1 + f_2 \bullet Y_{app}^2 + f_3 \bullet Y_{app}^3 + \dots + f_{n-1} \bullet Y_{app}^{n-1} \\ &= \sum_{i=1}^{n-1} f_i \bullet Y_{app}^i \end{aligned} \quad (10)$$

$$f_i = \frac{n_i}{n} \quad \sum_{j=1}^{n-1} n_j = n$$

and

$$\sum_{i=1}^{n-1} f_i = 1 \quad (11)$$

So the four-state, five-state unfolding curves can be fitted by using eq(10).

3. The unfolding free energy represented by the curve (Y_{app}^1) and the (Y_{app}^2) are $\Delta G_1^0(\text{H}_2\text{O})$ and $\Delta G_2^0(\text{H}_2\text{O})$, respectively, for structural elements E_1 and E_2 . Y_{app} is the unfolding curve of

protein which is consisted of structural elements, E_1, E_2 . Then the three-state unfolding free energy, $\Delta G_{total}^0(H_2O)$ represented by the curve (Y_{app}) can be calculated from $\Delta G_1^0(H_2O)$ and $\Delta G_2^0(H_2O)$ using the same molar fraction and eq(12).

$$\Delta G_{total}^0(H_2O) = n \cdot (f_1 \cdot \Delta G_1^0(H_2O) + f_2 \cdot \Delta G_2^0(H_2O)) \quad (12)$$

$$\frac{\Delta G_{total}^0(H_2O)}{n} = (f_1 \cdot \Delta G_1^0(H_2O) + f_2 \cdot \Delta G_2^0(H_2O))$$

If $\Delta G_2^0(H_2O)$ is greater than $\Delta G_1^0(H_2O)$, $\Delta G_{total}^0(H_2O) / n$ will change from $\Delta G_1^0(H_2O)$ to $\Delta G_2^0(H_2O)$. From eq(11) f_1 and f_2 can change from 0 to 1. The variation of $\Delta G_{total}^0(H_2O) / n$ with f_2 is shown in Figure 5.

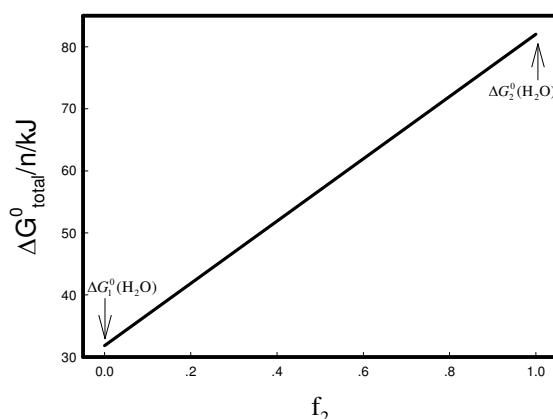


Fig. 5. The plot of $\Delta G_{total}^0(H_2O) / n$ against f_2 at 25°C. $\Delta G_1^0(H_2O) = 31.82 \text{ kJ mole}^{-1}$, $\Delta G_2^0(H_2O) = 82.01 \text{ kJ mole}^{-1}$.

Protein is consisted of structural elements, $E_1, E_2, E_3, \dots, E_{n-1}$, which appears $n_1, n_2, n_3, \dots, n_{n-1}$ times in the protein. The unfolding free energies corresponding to $E_1, E_2, E_3, \dots, E_{n-1}$ are $\Delta G_1^0(H_2O), \Delta G_2^0(H_2O), \Delta G_3^0(H_2O), \dots$, and $\Delta G_{n-1}^0(H_2O)$, respectively, and $\Delta G_i^0(H_2O) \neq \Delta G_j^0(H_2O)$, (i and j change from 1 to $n-1$). The unfolding free energy, $\Delta G_{total}^0(H_2O)$ of the protein can be calculated using eq(13).

$$\begin{aligned} \Delta G_{total}^0(H_2O) &= n \cdot (f_1 \cdot \Delta G_1^0(H_2O) + f_2 \cdot \Delta G_2^0(H_2O) + f_3 \cdot \Delta G_3^0(H_2O) + \\ &\quad + f_{n-1} \cdot \Delta G_{n-1}^0(H_2O)) \quad (13) \\ &= n \cdot \sum_{i=1}^{n-1} f_i \cdot \Delta G_i^0(H_2O) \end{aligned}$$

$$\frac{\Delta G_{total}^0(H_2O)}{n} = \sum_{i=1}^{n-1} f_i \cdot \Delta G_i^0(H_2O)$$

When n is 4 the four-state unfolding free energy, $\Delta G_{total}^0(H_2O) / n$ can be calculated from $\Delta G_1^0(H_2O), \Delta G_2^0(H_2O)$, and $\Delta G_3^0(H_2O)$. The plot of $\Delta G_{total}^0(H_2O)$ against f_1 and f_2 is shown in Figure 6.

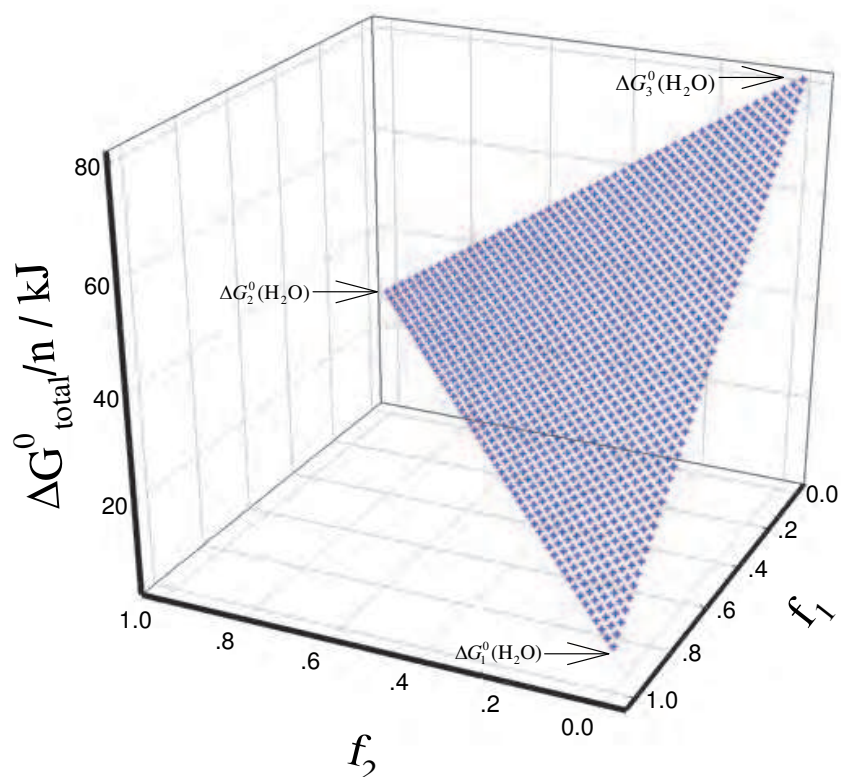


Fig. 6. The plot of $\Delta G_{total}^0(\text{H}_2\text{O})/n$ against the f_1 and f_2 at 25°C. $\Delta G_1^0(\text{H}_2\text{O}) = 10.56 \text{ kJ mole}^{-1}$, $\Delta G_2^0(\text{H}_2\text{O}) = 28.39 \text{ kJ mole}^{-1}$, and $\Delta G_3^0(\text{H}_2\text{O}) = 81.40 \text{ kJ mole}^{-1}$.

It can be seen that $\Delta G_{total}^0(\text{H}_2\text{O})/n$ is a point located at the plane consisted of $\Delta G_1^0(\text{H}_2\text{O})$, $\Delta G_2^0(\text{H}_2\text{O})$, and $\Delta G_3^0(\text{H}_2\text{O})$ in the space of $\Delta G_{total}^0(\text{H}_2\text{O})/n$, f_1 , and f_2 .

Although the unfolding curve of a protein, which is composed of same structural elements, i.e. E_i appears n times in the protein, is same with that of E_i , the $\Delta G_{protein}^0(\text{H}_2\text{O})$ of the protein is different with the $\Delta G_i^0(\text{H}_2\text{O})$ of E_i .

According to thermodynamics the $\Delta G_{Protein}^0(\text{H}_2\text{O})$ of the protein should be n times of the $\Delta G_i^0(\text{H}_2\text{O})$ of E_i (see eq(14)).

$$\Delta G_{Protein}^0(\text{H}_2\text{O}) = n \cdot \Delta G_i^0(\text{H}_2\text{O}) \quad (14)$$

3. Typical multistate unfolding curves

Three-state unfolding curves

From eq(8) three-state unfolding curve is dependence on $Y_{app}^1(m_1, [D]_{1/2}^1)$ and the $Y_{app}^2(m_2, [D]_{1/2}^2)$. Some typical three-state unfolding curves are given in Figure 7. When $m_1 = m_2$, and $[D]_{1/2}^1 \neq [D]_{1/2}^2$, the three-state unfolding curve is shown in Figure 7A. When $m_1 < m_2$, and $[D]_{1/2}^1 \neq [D]_{1/2}^2$, the three-state unfolding curve is shown in Figure 7B. And when $m_1 > m_2$, and $[D]_{1/2}^1 \neq [D]_{1/2}^2$, the three-state unfolding curve is shown in Figure 7C.

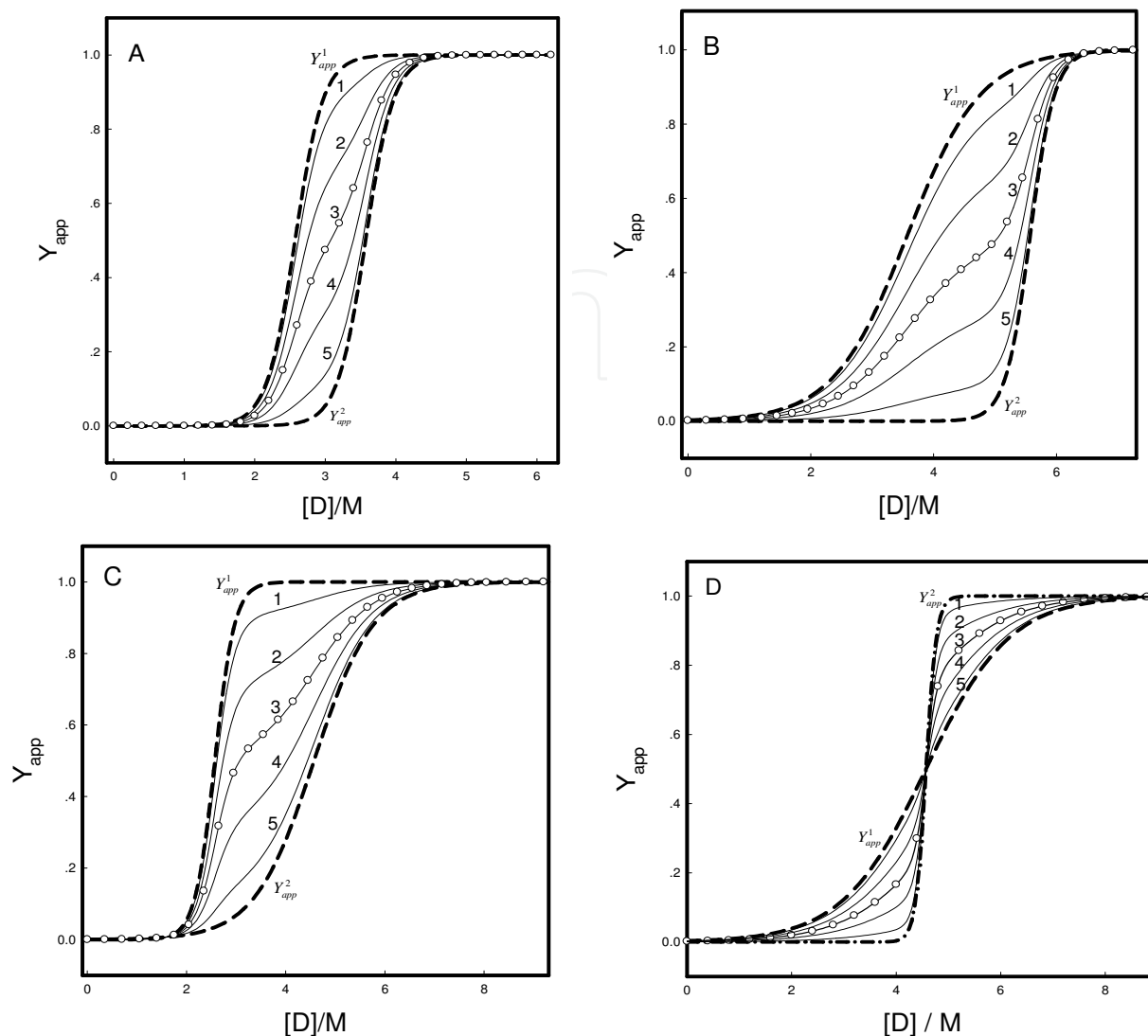


Fig. 7. Typical three-state unfolding curves. (○) represents measured value and Y_{app}^1 , Y_{app}^2 are the unfolding curves of structural elements E_1 and E_2 , respectively. Solid lines (1), (2), (3), (4) and (5) are the fitted based eq(8) for f_1 are 0.1, 0.3, 0.5, 0.7, and 0.9, respectively. A: $m_1 = m_2 = -24.72 \text{ kJ} \cdot \text{M}^{-1} \text{ mole}^{-1}$, $[D]_{1/2}^1 = 2.57\text{M}$, and $[D]_{1/2}^2 = 3.57\text{M}$; B: $m_1 = -4.13 \text{ kJ} \cdot \text{M}^{-1} \text{ mole}^{-1}$, $m_2 = -24.72 \text{ kJ} \cdot \text{M}^{-1} \text{ mole}^{-1}$, $[D]_{1/2}^1 = 3.57\text{M}$, and $[D]_{1/2}^2 = 5.57\text{M}$; C: $m_1 = -24.72 \text{ kJ} \cdot \text{M}^{-1} \text{ mole}^{-1}$, $m_2 = -4.13 \text{ kJ} \cdot \text{M}^{-1} \text{ mole}^{-1}$, $[D]_{1/2}^1 = 2.57\text{M}$, and $[D]_{1/2}^2 = 4.57\text{M}$; D: $m_1 = -2.48 \text{ kJ} \cdot \text{M}^{-1} \text{ mole}^{-1}$, $m_2 = -24.72 \text{ kJ} \cdot \text{M}^{-1} \text{ mole}^{-1}$, $[D]_{1/2}^1 = [D]_{1/2}^2 = 4.57\text{M}$

Of course, if the difference of $[D]_{1/2}^1$ and $[D]_{1/2}^2$ is greatly, stable intermediate state could be easily observed. When $m_1 < m_2$, and $[D]_{1/2}^1 = [D]_{1/2}^2$, the three-state unfolding curve is shown in Figure 7D. The unfolding curves in Figure 7D are often considered as two-state unfolding.

Four-state unfolding curves

When n is 4 the unfolding curve appears three transitions from eq(10). The four-state unfolding curve is a function of Y_{app}^1 , Y_{app}^2 , Y_{app}^3 , and f_i . Some typical four-state unfolding curves are shown in Figure 8.

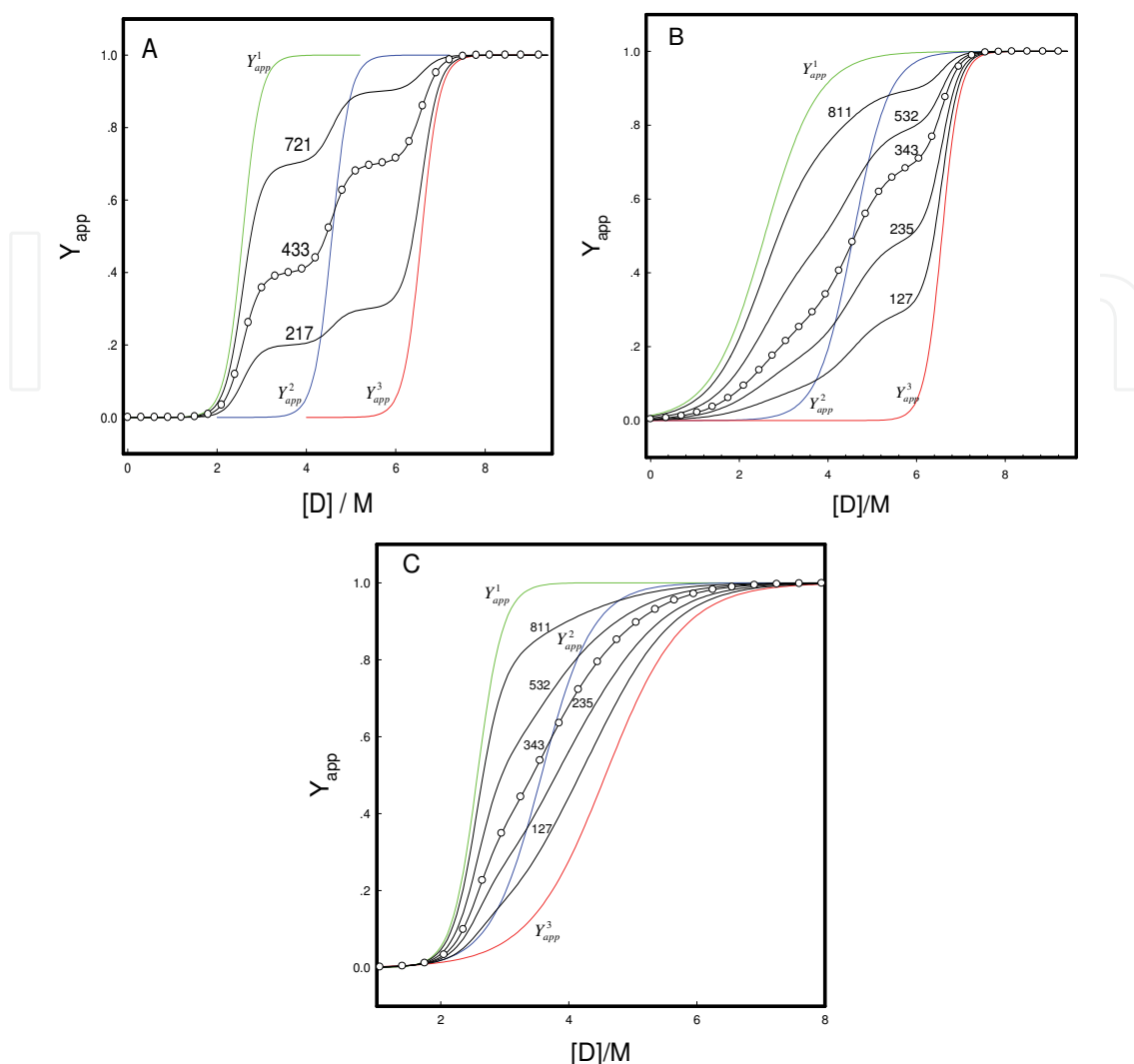


Fig. 8. Typical four-state unfolding curves. (○) represents measured value and Y_{app}^1 (green line), Y_{app}^2 (blue line), and Y_{app}^3 (red line), are the unfolding curves of structural elements E_1 , E_2 and E_3 , respectively. Solid lines labeled as l_{st} , representing f_1 as l tenth, f_2 as s tenth, and f_3 as t tenth, are the fitted based eq(10) when n is 4. A: $m_1 = m_2 = m_3 = -12.35 \text{ kJ} \cdot \text{M}^{-1} \cdot \text{mole}^{-1}$, $[D]_{1/2}^1 = 2.57\text{M}$, $[D]_{1/2}^2 = 4.57\text{M}$, and $[D]_{1/2}^3 = 6.57\text{M}$; B: $m_1 = -4.13 \text{ kJ} \cdot \text{M}^{-1} \cdot \text{mole}^{-1}$, $m_2 = -6.19 \text{ kJ} \cdot \text{M}^{-1} \cdot \text{mole}^{-1}$, and $m_3 = -12.35 \text{ kJ} \cdot \text{M}^{-1} \cdot \text{mole}^{-1}$, $[D]_{1/2}^1 = 2.57\text{M}$, $[D]_{1/2}^2 = 4.57\text{M}$, and $[D]_{1/2}^3 = 6.57\text{M}$; C: $m_1 = -12.35 \text{ kJ} \cdot \text{M}^{-1} \cdot \text{mole}^{-1}$, $m_2 = -6.19 \text{ kJ} \cdot \text{M}^{-1} \cdot \text{mole}^{-1}$, and $m_3 = -4.13 \text{ kJ} \cdot \text{M}^{-1} \cdot \text{mole}^{-1}$, $[D]_{1/2}^1 = 2.57\text{M}$, $[D]_{1/2}^2 = 3.57\text{M}$, and $[D]_{1/2}^3 = 4.57\text{M}$.

4. Structural element

Structural element is a smallest structural unit in native protein, of which the unfolding obeys two-state model.

Native proteins are only marginally entities under physiological conditions. There are various no covalent bonds to which protein is subject—electrostatic interactions (both attractive and repulsive), hydrogen bonding (both intramolecular and to water), and

hydrophobic force, over an entire protein molecule. The low conformational stabilities of native proteins make them easily susceptible to denaturation by altering the balance of the weak nonbonding forces that maintain the native conformation. Native protein structure unfolds in a highly cooperative manner: Any partial unfolding of the structure destabilizes the remaining structure, which must simultaneously collapse to the random coil.

It has been shown that the unfolding or folding of small globular proteins occurs via a two-state process, whereas the unfolding or folding of larger proteins is complex and often involves the formation of intermediate [9]. Thioredoxin is characterized by an active site containing two cysteine residues separated by two other residues. The reversible oxidation of these cysteine residues to the disulfide form serves as a redox couple for a number of biological reactions. It was first characterized in yeast for its role in the reduction of methionine sulfoxide and inorganic sulphate [10, 11]. The backbone of oxidized form and ribbon model of reduced form for *Escherichia coli* thioredoxin are shown in Figure 9. The protein consists of single polypeptide chain of 108 amino acid residues. Either the oxidized or the reduced forms the protein is a compact molecule with 90% of its residues in α -helices, β -strands or reverse turns, which a core of twisted β -strand is flanked on either side by α -helices. The conversion between the oxidized and the reduced forms is accompanied by a change in conformation that is reflected in the fluorescence properties of Trp28.

The equilibrium unfolding of the oxidized form of *Escherichia coli* thioredoxin at pH 7 was studied by Santoro and Bolen [1] using guanidine hydrochloride (GdnHCl) and urea as denaturant at 25°C by monitoring the changes in ellipticity at 222nm.

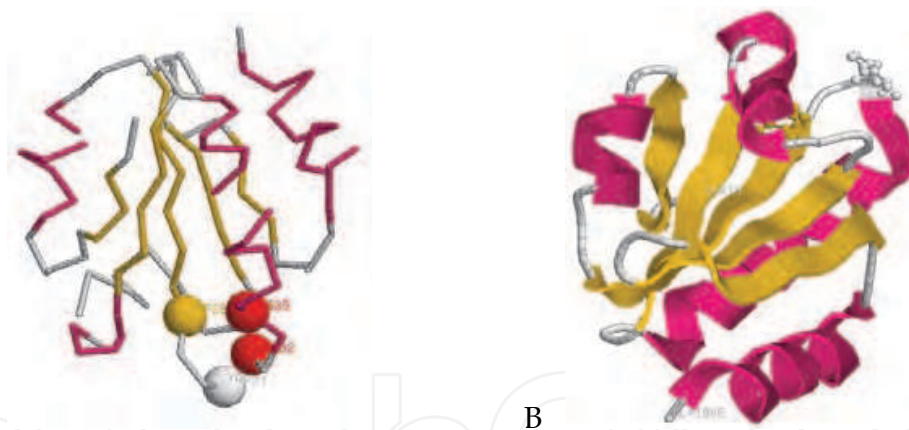


Fig. 9. Backbone of oxidized form (A) and Ribbon model of reduced form (B) for *E coli* thioredoxin. The figures were generated using the Protein Data Bank files 1SRX and 2TRX, respectively. Trp residues are indicated as ball and stick, α -helices (pink) and β -strands (yellow) are shown.

The GdnHCl- or urea-induced unfolding of thioredoxin is a two-state process. The unfolding free energy change is 7.8 ± 0.2 kcal/mole (32.64 ± 0.84 kJ/mole) in the absence of (GdnHCl) or 8.6 ± 0.9 kcal/mole (35.98 ± 3.77 kJ/mole) in the absence of urea. Thermal unfolding measurements give $\Delta G^0(\text{H}_2\text{O})$ being 8.1 ± 0.1 kcal/mole (33.89 ± 0.42 kJ/mole) by using differential scanning calorimetry. Within error, $\Delta G^0(\text{H}_2\text{O})$ values obtained from GdnHCl- and urea-induced, and thermal unfolding are in agreement, meaning that GdnHCl, urea, and thermal unfolding involve the same native form to unfolding form equilibrium in oxidized form of *Escherichia coli* thioredoxin.

The free energy required to denature a protein is ~ 0.4 kJ/mole of amino acid residues so that 100-residue protein is typically stable by only around 40 kJ/mole [12]. Since the measured $\Delta G^0(\text{H}_2\text{O})$ of thioredoxin is close to 40 kJ/mole, the compact protein molecule can be considered as a structural element.

Goat β -lactoglobulin consists of single polypeptide chain of 101 amino acid residues. The protein contains α - helices (red) and β - sheets (yellow) as shown in Figure 10. The measured $\Delta G^0(\text{H}_2\text{O})$ is 11.7 ± 0.8 kcal/mole (48.95 ± 3.35 kJ/mole) at 25°C by measuring optical rotation [13]. β -lactoglobulin can be considered as a structural element. Although α -chymotrypsin consists of single polypeptide chain of 178 amino acid residues the $\Delta G^0(\text{H}_2\text{O})$ is only 8.3 ± 0.4 kcal/mole (34.73 ± 1.67 kJ/mole) at 25°C by measuring optical rotation [13]. If the $\Delta G^0(\text{H}_2\text{O})$ of a 100-residue protein were 40 kJ/mole, the $\Delta G^0(\text{H}_2\text{O})$ of α -chymotrypsin would have been around 70 kJ/mole at 25°C . It means that α -chymotrypsin contains same structural elements at least two.

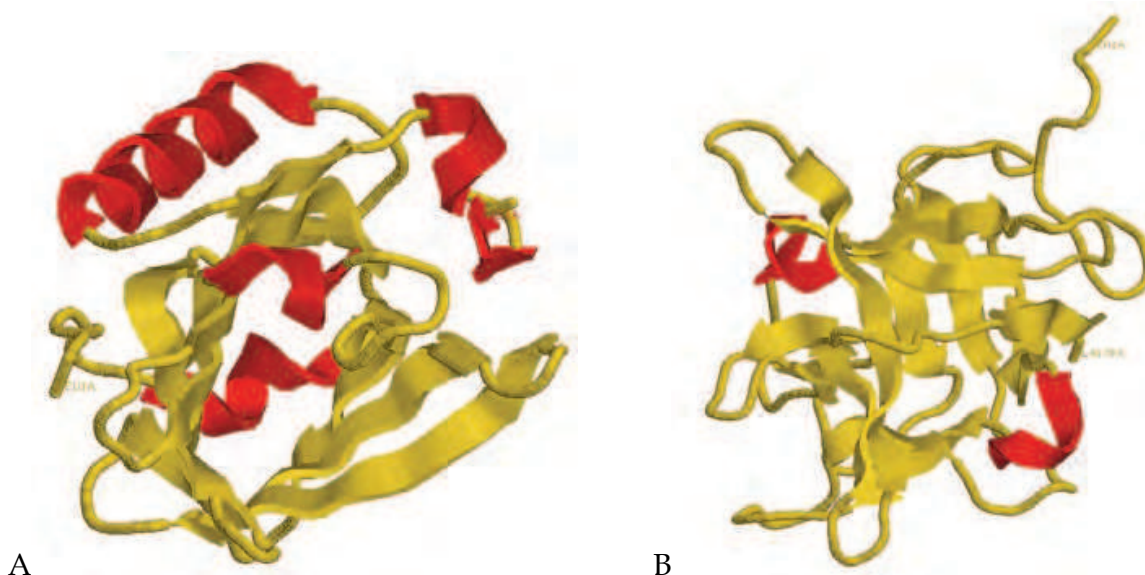


Fig. 10. Ribbon models of β -lactoglobulin (A) and α -chymotrypsin (B). The figures were generated using the Protein Data Bank files 3NPO and 1XG6, respectively. α - helices (red) and β - strands (yellow) are shown.

Human serum albumin (HSA) has been used as a model protein for protein folding and ligand-binding studies over many decades [5, 14-19]. The protein is a single chain protein with 585 amino acids, with a molecular weight of $\sim 67,000$ Da. Serum albumin homologs with very similar properties are found in other mammals. The protein contains only α -helices. The structure of this protein has been determined by X-ray crystallography of high resolution (Figure 11); it includes three homologous domains (I-III) that assemble a heart-shaped molecule. Each domain is formed by two subdomains that possess common structural motifs. Only one cysteine residue located at position 34 (in domain I) with a free sulfhydryl group. HSA plays a special role in transporting metabolites and drugs throughout the vascular system and also in maintaining the pH and osmotic pressure of plasma. Interestingly, the structure and dynamics of HAS are known to be influenced by a number of factors, like pH, temperature, and binding of different ligands.

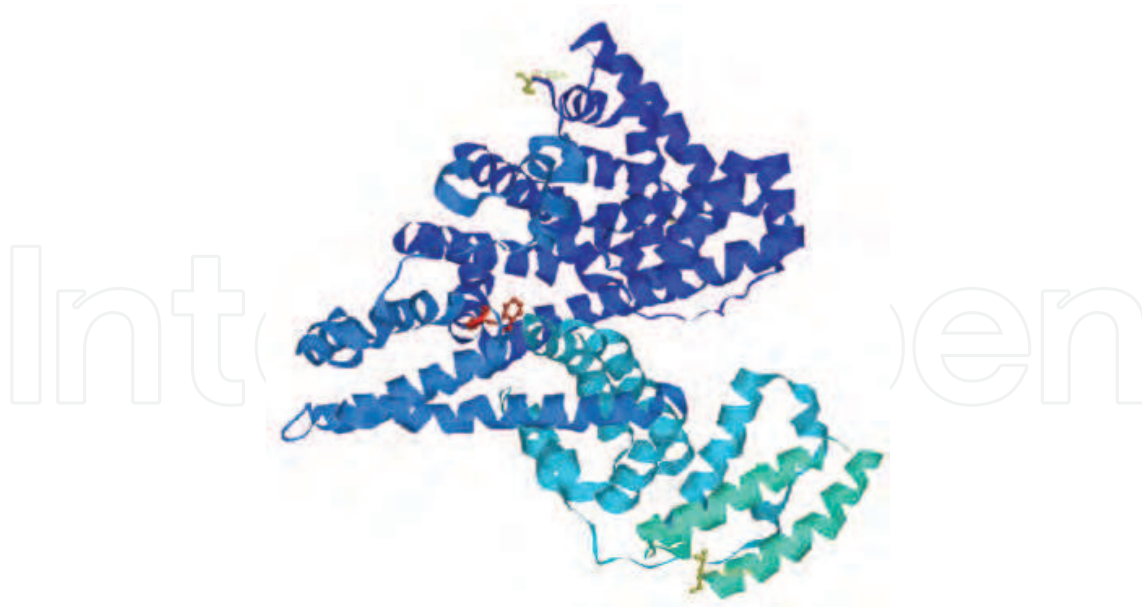


Fig. 11. Structure of human serum albumin (PDB: 1BJ5). Trp residue at 214 is indicated as ball and stick in red.

Denaturation of HSA has been studied by several workers using different methods like absorption difference at 287nm, fluorescence at 340nm upon excitation at 282nm, tryptophan fluorescence upon excitation at 295nm, ellipticity at 222nm, 1-anilinonaphthalene-8-sulfonate fluorescence, differential calorimetry, etc. Denaturation of HSA has been suggested to follow a single-step transition as well as two- or multiple-step transitions depending upon the reaction conditions and probes used. For example, urea denaturation of HSA has been shown to follow a two-step, three-state transition involving one intermediate when studied by fluorescence and ellipticity measurements but became single-step, two-state transition when studied by UV difference spectroscopy. Similarly, guanidine hydrochloride (GdnHCl) denaturation of serum albumin has been reported to follow both single-step and two-step transitions [16]. Meanwhile the measured $\Delta G^0(\text{H}_2\text{O})$ has big difference. The measured $\Delta G^0(\text{H}_2\text{O})$ is 5.98 kcal/mole (25.02 kJ/mole) and 6.00 kcal/mole (25.10 kJ/mole) at 25°C, 1M KCl pH 7.0 by measuring circular dichroism and fluorescence, respectively [5]. In the presence of 2,2,2-trifluoroethanol the measured $\Delta G^0(\text{H}_2\text{O})$ is 8.04 kcal/mole (33.64 kJ/mole) and 8.06 kcal/mole (33.72 kJ/mole) [15]. 2,2,2-trifluoroethanol makes the $\Delta G^0(\text{H}_2\text{O})$ increase around 2 kcal/mole. Halim et al [16] used bromophenol blue as a probe the $\Delta G^0(\text{H}_2\text{O})$ of bovine serum albumin is 4.04 and 4.60 kcal/mole, respectively, from urea and GdnHCl two-state denaturation curves at pH 8.0, 25°C. However, the $\Delta G^0(\text{H}_2\text{O})$ of HSA is 146.7 kJ/mole from sodium dodecyl sulphate two-state denaturation curves at pH 7.0, 35°C [17]. It means that HAS is a multi-element protein. When the structural elements are same at the experimental conditions the unfolding of HAS is a two-state process, and when the structural elements are different at another experimental conditions the unfolding behaves as a three-state process.

Urea-induced unfolding of bovine serum albumin and one of its fragments containing domain II+III has been studied by difference spectral and fluorescence emission measurements. The unfolding-refolding curves of both the proteins showed the presence of at least one stable intermediate when the transition was monitored at 288 nm. The presence

of the intermediate was not detectable at 293 nm where only tryptophan contributed towards the protein absorption. However, both the proteins did show the presence of intermediate when the denaturation was monitored fluorometrically. Since domain III of the albumin is devoid of tryptophan, it is concluded that the formation of intermediate in the unfolding-refolding transition of serum albumin involves (i) unfolding of domain III, (ii) minor structural transformations in domain II, and/or (iii) the separation of the sub-domains of domain III from each other [15-17].

5. The factors affected structural element

Acquisition of native globular conformation (3D structure) of a protein is governed by its structural elements and biological environment surrounding it. The stability of protein's 3D structure is endorsed by various intramolecular forces, such as hydrogen bonds, van der Waals, electrostatic and hydrophobic interactions involving various amino acid side chains as well as their milieu in the native structure. So protein structure is affected by factors such as experiment conditions (extreme temperature, pH and pressure) and presence of destabilizing agents (salt, alkali, denaturant and surfactant), and of stabilizing agents (metal ions, anions and small organic molecules) [15-19]. In fact they are the factors which structural element is affected. A few examples are given to show the effect of stabilizing agents on structural element.

Anticoagulation factor I (ACF I) isolated from the venom of *Agkistrodon acutus* is an activated coagulation factor X-binding protein in a Ca^{2+} -dependent fashion with marked anticoagulant activity. The protein is a single chain protein with 129 amino acids, in which there are 7 Trp. The crystal structure measurement shows that the protein has both α -helices and β -sheets and tryptophan residues locate at α -helices, β -sheets and loops. Metal ions-induced stabilization and unfolding of ACF I was studied in guanidine hydrochloride solutions by Xu et al [6] following the fluorescence and circular dichroism. Metal ions can increase the structural stability of ACF I against guanidine hydrochloride denaturation and change its unfolding behavior. Reproduced unfolding curves of apo-ACF I and holo-ACF I from ref [6] are shown in Figure 12.

| Holo-ACF I | F \leftrightarrow Ia | [D] _{1/2} /M | | -m/(kcal/M/mole) | | |
|---------------------------|------------------------|-------------------------|------------------------|------------------------|-------------------------|------------------------|
| | | Ia \leftrightarrow Ib | Ib \leftrightarrow U | F \leftrightarrow Ia | Ia \leftrightarrow Ib | Ib \leftrightarrow U |
| Unfolding | 0.66 \pm 0.02 | 1.60 \pm 0.04 | 2.52 \pm 0.05 | 3.76 \pm 0.09 | 3.63 \pm 0.04 | 2.59 \pm 0.02 |
| Refolding | 0.67 \pm 0.03 | 1.59 \pm 0.02 | 2.55 \pm 0.06 | 3.70 \pm 0.05 | 3.79 \pm 0.10 | 2.77 \pm 0.08 |
| ΔG^0 /(kcal/mole) | | | | | | |
| Holo-ACF I | F \leftrightarrow Ia | Ia \leftrightarrow Ib | Ib \leftrightarrow U | total | | |
| Unfolding | 2.51 \pm 0.04 | 2.21 \pm 0.02 | 1.29 \pm 0.03 | 6.01 \pm 0.09 | | |
| Refolding | 2.60 \pm 0.07 | 2.16 \pm 0.03 | 1.31 \pm 0.02 | 6.07 \pm 0.12 | | |

Table 1. Thermodynamic parameters for unfolding and refolding of ACF I by GdnHCl at 25°C, monitored by measurement of fluorescence at 340nm

The guanidine hydrochloride induced unfolding of apo-ACF I is a two-state process with no detectable intermediate state, whereas the unfolding of holo-ACF I follows a three-step transition, with intermediate state Ia and intermediate state Ib. The thermodynamic parameters for unfolding and refolding of ACF I are shown in Table 1 [6]. The unfolding

data can be fitted by using eq (3) for two-state process of apo-ACF I and eq (10) for four-state process of holo-ACF I, respectively.

Using the new method it can be thought that ACF I is consisted of multi-structural elements, and the structural elements are same in apo-ACF I in guanidine hydrochloride. The stability of structural element can be described by parameters $[D]_{1/2}$ (1.22M) and m (-4.06 kcal/M/mole), i.e. $\Delta G^0(\text{H}_2\text{O})$ is 4.96 kcal/mole. After binding Ca^{2+} the structural elements are changed. At least three-kind structural elements appear in holo-ACF I. Their stability is 4.22 kcal/mole, 7.07 kcal/mole, and 5.95 kcal/mole, for structural element 1, 2, and 3, respectively.

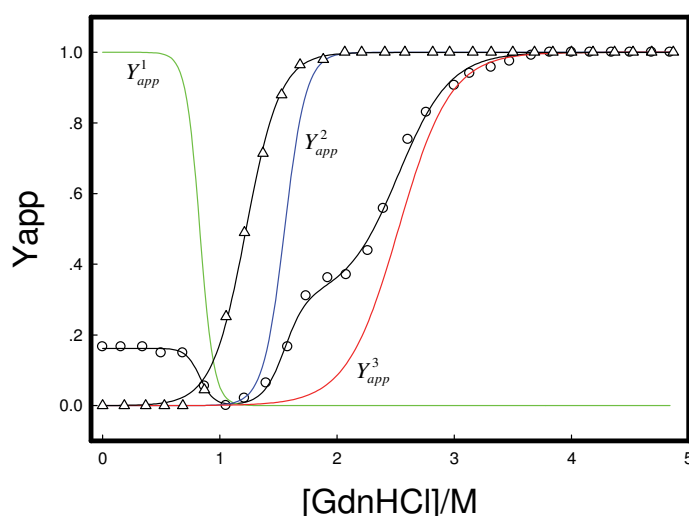


Fig. 12. Guanidine hydrochloride (GdnHCl)-induced unfolding of anticoagulation factor I (ACF I) in 0.02 M Tris-HCl buffer (pH 7.6, 25°C). Unfolding transitions of apo-ACF I(Δ), and holo-ACF I(\circ) monitored by measurement of fluorescence at 340 nm after exciting at 295 nm. The data were reproduced from ref [6]. Black lines are the fitting from eq (3) corresponding to two-state process and eq (10) corresponding to four-state process, respectively. The unfolding transition of structural element is shown as Y_{app}^1 (green), Y_{app}^2 (blue), and Y_{app}^3 (red), respectively.

Parameters of $[D]_{1/2}$ and m values are 0.85M and -4.96 kcal/M/mole, 1.56M and -4.53 kcal/M/mole, 2.56M and -2.32 kcal/M/mole, for structural element 1, 2, and 3, respectively. The unfolding of holo-ACF I Y_{app} can be fitted from eq (10).

$$Y_{app} = 0.14 \times Y_{app}^1 + 0.26 \times Y_{app}^2 + 0.60 \times Y_{app}^3 \quad (15)$$

where Y_{app}^1 , Y_{app}^2 , and Y_{app}^3 are unfolding transition of structural element 1, 2, and 3, respectively.

The $\Delta G_{total}^0(\text{H}_2\text{O})/n$ of holo-ACF I is 6.00 kcal/mole from eq (13).

$$\begin{aligned} \frac{\Delta G_{total}^0(\text{H}_2\text{O})}{n} &= 0.14 \times \Delta G_1^0(\text{H}_2\text{O}) + 0.26 \times \Delta G_2^0(\text{H}_2\text{O}) + 0.60 \times \Delta G_3^0(\text{H}_2\text{O}) \\ &= 0.14 \times 4.22 + 0.26 \times 7.07 + 0.60 \times 5.95 = 6.00 \end{aligned} \quad (16)$$

If using the stability of structural element in apo-ACF I as standard the binding of Ca^{2+} makes structural element 1 be destabilized and 2 and 3 be stabilized. Of the various forces, hydrogen bonding and hydrophobic effect have been shown to make significant contribution to the protein stability. Being secondary contributor to protein's stability through salt bridges, charged residues have also been found important in manipulating protein stability [20]. It is that Ca^{2+} binding breaks the balance of charged residues makes the charged residues in apo-ACF I re-distribute and form new structural elements in holo-ACF I.

Second example is succinylation-induced conformational destabilization of lysozyme as studied by guanidine hydrochloride denaturation [20]. Figure 13 shows the crystal structure of lysozyme which is made up of a single polypeptide chain of 129 amino acid residues arranged in the form of two domains and stabilized by four disulphide bonds. All six lysine residues are distributed in the molecular surface and all six tryptophan residues are located at α -helices and loops. The unfolding of the protein obeys two-state process, meaning that the protein is consisted of same structural element(s). Using fluorescence data upon excitation at 280nm value of $\Delta G_{total}^0(\text{H}_2\text{O})/n$ is 8.56 kcal/mole and 'm' is -2.03kcal/M/mole for native lysozyme. When excitation at 295nm $\Delta G_{total}^0(\text{H}_2\text{O})/n$ is 7.96 kcal/mole and 'm' is -1.93 kcal/M/mole. Using 100-fold molar excess of succinic anhydride, about 99% of lysine residues of lysozyme were modified. Though the succinylated lysozyme obeys two-state process yet a pronounced decrease in $\Delta G_{total}^0(\text{H}_2\text{O})/n$ value is noticed with succinylated lysozyme preparation compared to native lysozyme. $\Delta G_{total}^0(\text{H}_2\text{O})/n$ value is 4.40 kcal/mole and 4.67 kcal/mole excitation at 280nm and 295nm, respectively. The 'm' values are also changed from -2.03 kcal/M/mole and -1.93 kcal/M/mole (for native lysozyme) to -1.54 kcal/M/mole and -1.59 kcal/M/mole for succinylated lysozyme, respectively. The conformational destabilization of the modified protein can be attributed to the effect of succinylate on structural element(s), i.e. it is that the positive charges on lysine residues are neutralized by negative charges on succinylate, makes the structural element(s) be destabilized. Experimental measurements show that the net charge of both native and succinylated lysozyme is +8 and -9, respectively at pH 7.0.



Fig. 13. Ribbon model of lysozyme produced with a Protein Data Bank file 1VDQ. Trp residues are indicated as wireframe and Lys residues are shown as ball and stick.

Third example is HAS, whose crystal is shown in Figure 11. In the presence of different concentrations of KCl urea-induced denaturation of HAS displays different pathways. When the concentration of KCl is 1.0M HAS undergoes a single-step transition with no intermediate. At pH 7.0, 25°C the variation of ΔG as a function of urea concentration is presented in Figure 14A (curve 2). According to eq (5) $\Delta G_{total}^0(\text{H}_2\text{O})/n$ and 'm' values can be obtained to be 5.98 ± 0.26 kcal/mole and $-(1.03 \pm 0.04)$ kcal/M/mole, respectively. In the absence of KCl the unfolding of HAS is a two-step transition process and the urea-induced denaturation curve is shown in Figure 14B, using the data of Figure 1B or 1A in ref [5]. Muzammil et al [5] considered that first transition corresponded to the formation of intermediate state whereas second transition corresponded to the unfolding of the intermediate. Assuming both the transitions follow two-state mechanism the variations of ΔG as a function of urea concentration are presented in Figure 14A (curve 1 and 3) at pH 7.0, 25°C. According to eq (5) $\Delta G_1^0(\text{H}_2\text{O})$ and $\Delta G_2^0(\text{H}_2\text{O})$ are 3.66 ± 0.35 kcal/mole and 5.38 ± 0.24 kcal/mole, respectively. The 'm' values are $-(0.95 \pm 0.10)$ kcal/M/mole and $-(0.80 \pm 0.04)$ kcal/M/mole, respectively. From eq (6) the $[D]_{1/2}$, of which corresponds second transition from intermediate state to unfolding state, should be 6.73M. However, the authors [5] reported $\Delta G_2^0(\text{H}_2\text{O})$ to be 1.4 kcal/mole. Using 'm' value as -0.80 kcal/M/mole the calculated $[D]_{1/2}$ is only 1.75M from eq (6). The difference of $[D]_{1/2}$ is 4.98 M, at which the second transition from intermediate state to unfolding state starts. The authors [5] got $\Delta G_2^0(\text{H}_2\text{O})$ from extrapolation of ΔG values upto the starting of second transition. Since $\Delta G_{total}^0(\text{H}_2\text{O})/n$ being a thermodynamic property does not depend on the path free energy change in the absence of salt should be obtained by summing the $\Delta G_1^0(\text{H}_2\text{O})$ and $\Delta G_2^0(\text{H}_2\text{O})$. The $\Delta G_{total}^0(\text{H}_2\text{O})/n$ (4.89 kcal/mole) in the absence of KCL is smaller than that (5.98 kcal/mole) in the presence of 1M KCl. The authors attributed the binding of Cl⁻ to the domain III to stabilize the domain [5].

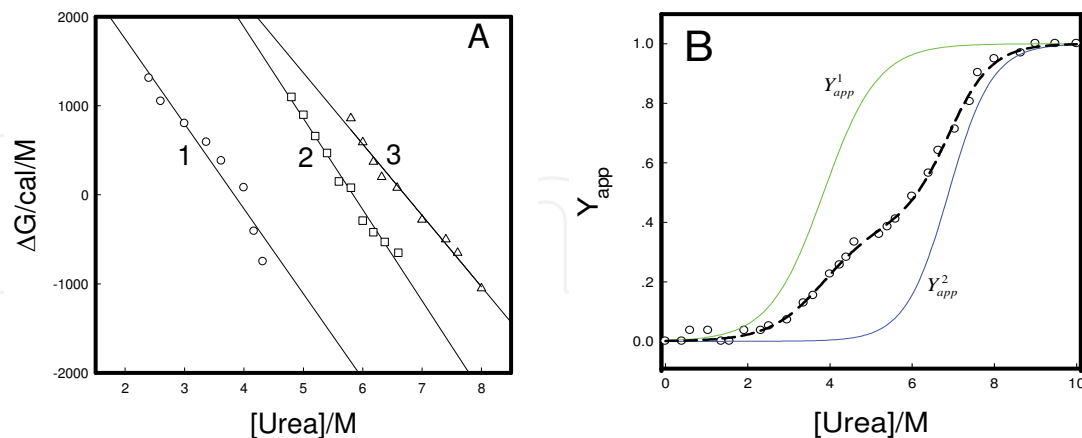


Fig. 14. Urea-induced unfolding of HAS at pH 7.0, 25°C in the presence as well as absence of KCl. A: Dependence of free energy change on urea concentration for the transitions (1): F \leftrightarrow I; (2): F \leftrightarrow U; and (3): I \leftrightarrow U. B: Normalized curve for the transition F \leftrightarrow U in the absence of KCl. Data (○) obtained from the Figure 2 in ref [5]. Medium dash is the fitting from eq (8), Y_{app}^1 (green) and Y_{app}^2 (blue) are unfolding transition of structural element 1 and 2, respectively.

In my views the calculation of $\Delta G_2^0(\text{H}_2\text{O})$ is unreasonable. $\Delta G^0(\text{H}_2\text{O})$ is a parameter to describe the stability of a protein. In two-state transition 'm' and $[\text{D}]_{1/2}$ values are also two parameters to describe the stability of the protein. When 'm' is same the $\Delta G^0(\text{H}_2\text{O})$ is proportional to $[\text{D}]_{1/2}$. The protein whose unfolding curve appears at higher denaturant concentrations is more stable than that whose unfolding curve appears at lower denaturant concentrations. For the unfolding curve of HAS (Figure 14B) in the absence of KCl, two transitions are observed. The first transition starts at around 2M urea and completes at 4.5M urea, and the second transition starts at around 5.2M urea and finally slopes off at 8.4M urea. The free energy change corresponded to second transition is greater than that corresponded to the first transition if 'm' is nearly same. The reported $\Delta G_2^0(\text{H}_2\text{O})$ (=1.40 kcal/mole) < $\Delta G_1^0(\text{H}_2\text{O})$ (=3.40 kcal/mole) [5]. Using the new method HAS is consisted of multi-structural elements. In the absence of KCl HAS contains at least two-kind structural elements, the unfolding shows three-state process. A least squares analysis of the data in Figure 14B according to eq (8) yielded a fitting curve, Y_{app} .

$$Y_{app} = 0.40 \times Y_{app}^1 + 0.60 \times Y_{app}^2 \quad (17)$$

where Y_{app}^1 and Y_{app}^2 are unfolding transition of structural element 1 and 2, respectively. According eq (12) the $\Delta G_{total}^0(\text{H}_2\text{O})/n$ express as

$$\begin{aligned} \frac{\Delta G_{total}^0(\text{H}_2\text{O})}{n} &= 0.40 \times \Delta G_1^0(\text{H}_2\text{O}) + 0.60 \times \Delta G_2^0(\text{H}_2\text{O}) \\ &= 0.40 \times 3.66 + 0.60 \times 5.38 = 4.69 \end{aligned} \quad (18)$$

The $\Delta G_{total}^0(\text{H}_2\text{O})/n$ (4.69 kcal/mole) in the absence of KCl is smaller than that (5.98 kcal/mole) in the presence of 1M KCl. The binding of Cl⁻ to the domain III to stabilize the domain

6. The unfolding of CopC

The protein CopC of *Pseudomonas syringae* pathovar tomato (CopC) is one of four proteins, CopA, B, C, and D, coded on the copper resistance operon (cop). CopC belonging to periplasmic protein, consists of 102 amino acids. In solution it adopts a fold essentially constituted by nine β sheets forming a barrel motif. The copper (I) site located in C-terminal is constituted by His-48 and two or three of the four Met residues (40, 43, 46, 51) $[\text{Cu}^{\text{I}}(\text{His})(\text{Met})_x]$ ($x = 2$ or 3). On the other hand, the protein is known to bind copper (II) in an N-terminal position that is found consistent with a coordination arrangement including His-1, Glu-27, Asp-89, and His-91 $[\text{Cu}^{\text{II}}(\text{His})_2(\text{Asp})(\text{Glu})(\text{OH}_2)]$. They represent novel coordination environments for copper in proteins and the two copper binding sites are about 30 Å apart. All of these have been confirmed by the method of nuclear magnetic resonance (NMR) and extended X-ray absorption fine structure spectroscopy (EXAFS) [21, 22]. CopC has high affinity for both copper ions although the Cu(II) site has the highest affinity ($\sim 10^{13} \text{ M}^{-1}$) [23, 24]. The binding sites of CopC can also occupied by other transition metal ions. However the affinity is lower than copper ions. For example, Hg(II) ions can bind to the both sites [25] and Ag(I) only binds to the Cu(I) site [26]. Figure 15 shows the NMR structure of apoCopC (A) and crystal structure of Cu^{2+} -CopC- Cu^+ (B) drawn with the

Protein Data Bank files 1M42 and 2C9Q, respectively. A β -sandwich structure comprised of β -strands arranged in a Greek Key topology exists in apoCopC and Cu^{2+} -CopC- Cu^+ . Single tryptophan residue 83, sandwiched between the two β sheets, locates at a rather hydrophobic microenvironment and has numerous contacts with residues in strand $\beta 2$ and strand $\beta 7$ [27].

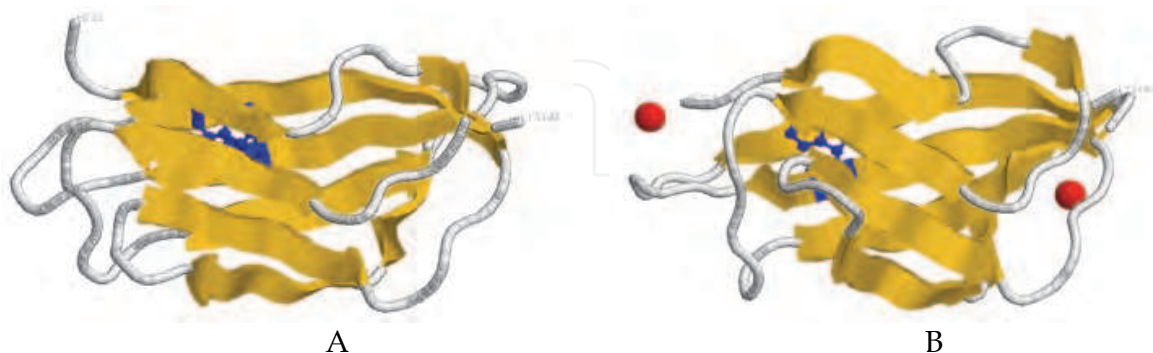


Fig. 15. NMR structure of apoCopC (1M42) (A) and crystal structure of Cu^{2+} -CopC- Cu^+ and (2C9Q) (B) revealing the β -sandwich fold, at which Trp (blue) locates and Cu(II), Cu(I) (red).

The fluorescence properties of tryptophan residues in protein can be considered as three discrete spectral classes: One is the buried in nonpolar regions of the protein, the fluorescence maximum position appears at 310~330 nm and spectral band width is around 48~49 nm; two is located at the surface of protein and completely exposed to water, maximum peak is in 350~353 nm and half bandwidth is in the range of 59~61 nm; the latter is in limited contact with water which is probably immobilized by bonding at the macromolecular surface, the fluorescence maximum peak is located at 340~342 nm and the half bandwidth is about 53~55 nm.

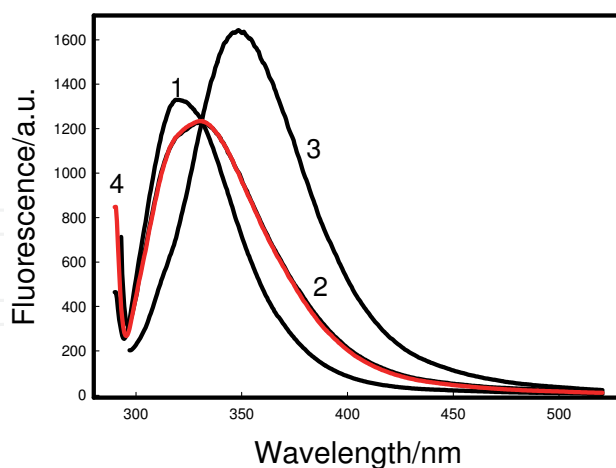


Fig. 16. Fluorescence spectra of apoCopC in the absence or presence of urea, in 20 mM PBS and 0.1 M NaCl, pH 6.0. The concentration of urea / M is 1: 0; 2: 5; 3: 9.4, respectively. 4 is the fitted curve according to two-state mechanism.

Figure 16 is the spectra of apoCopC in different experimental conditions. In the presence of 9.4 M urea the fluorescence peak of apoCopC locates at 353 nm and the half bandwidth reaches to 60 nm (Figure 16 spectrum 3), meaning that apoCopC exists in unfolding state. In

the absence of urea the fluorescence peak of native apoCopC appears at 320 nm and the half bandwidth is 48 nm (Figure 16 spectrum 1), meaning that the tryptophan residue 83 is buried in nonpolar regions of apoCopC. In the presence of 5.0 M urea the fluorescence peak appears at 331 nm and the half bandwidth reaches to 66 nm (Figure 16 spectrum 2).

Obviously spectrum 2 is the summing of spectra produced by two-class tryptophan residue in protein(s). With the increasing of urea concentration an iso-fluorescence point keeps at 332nm from spectrum 1 to spectrum 3, meaning that there are two species of apoCopC in the presence of 5.0 M urea. Curve 4 (red line) in Figure 16 is fitted from spectrum 1 and 2, in which the contribution of spectrum 1 is 0.73 and that of spectrum 2 is 0.27. It can be seen that the fitted curve is nearly coincided with the measured spectrum. In the presence of 5.0 M urea apoCopC exists in native and completed unfolding forms. The fluorescence property of tryptophan residue 83 in apoCopC is an index to show the protein in either native or unfolding states. It can be deduced that the unfolding of apoCopC would obeys two-state mechanism.

When the tryptophan residue 83 is mutated as leucine residue the protein is nearly immeasurable by fluorescence. Meanwhile the mutagenesis make the ability of binding to Cu(II), the thermal stability of apoCopC be decreased [28]. The important role of the tryptophan residue 83 is not only in using as a fluorescence probe but also in keeping the β -sandwich hydrophobic structure. The thermodynamic stability apoCopC can be investigated at pH 7.4 by monitoring the fluorescence intensity at around 405 nm [25, 29, 30]. As known Cu^{2+} -CopC and Hg^{2+} -CopC- Hg^{2+} are prepared by adding Cu(II) or Hg(II). The unfolding of apoCopC, Cu^{2+} -CopC and Hg^{2+} -CopC- Hg^{2+} are reversible. According to two-state model, the free energy change can be measured, respectively, and the order of stability is Cu^{2+} -CopC \gg Hg^{2+} -CopC- Hg^{2+} \sim apoCopC. The binding of Cu(II) makes the stability of CopC be increased greatly. Although Hg(II) can also binding the Cu(II) site the contribution to the stability can be neglected. The reason is the weak binding of Hg(II) to the sites of apoCopC.

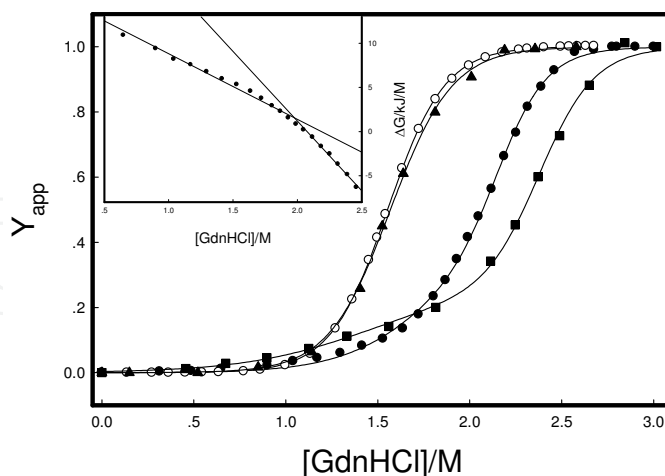


Fig. 17. GdnHCl-induced unfolding of CopC by monitoring the fluorescence 400/320 nm ratio for apoCopC (\circ), Cu^{2+} -CopC (\bullet), CopC- Ag^+ (\blacktriangle), and Cu^{2+} -CopC- Ag^+ (\blacksquare) forms at pH 7.4, 25°C. The solid lines are fitting curves in terms of two-state mechanism for apoCopC (\circ) and CopC- Ag^+ (\blacktriangle), of three-state for Cu^{2+} -CopC (\bullet) and Cu^{2+} -CopC- Ag^+ (\blacksquare) from eq (2) and eq (8), respectively. Inset: Dependence of free energy change of Cu^{2+} -CopC (\bullet) on GdnHCl concentration.

Using guanidine hydrochloride as chemical denaturant the unfolding profiles are presented in Figure 17 by monitoring the changes of fluorescence ratio at 400nm and 320nm. ApoCopC unfolds in two-state equilibrium reaction. It means that apoCopC is consisted of a kind of structural element(s). The $\Delta G^0(\text{H}_2\text{O})/n$, $[D]_{1/2}$ and 'm' values are listed in Table 2. When used urea as denaturant the obtained parameters are also in Table 2. Compared the data in Table 2 the $\Delta G^0(\text{H}_2\text{O})/n$ values agree between guanidine hydrochloride and urea as chemical denaturant. The unfolding curve of CopC-Ag⁺ roughly is a repeat of that of apoCopC. Like Hg(II), the binding of Ag(I) to the Cu(I) site of apoCopC does not also make the stability of the protein be increased. In another word, the structural element(s) in apoCopC don't affected by the binding of Hg(II) or Ag(I). The corresponding GdnHCl-induced unfolding with Cu²⁺-CopC reveals some difference. If the unfolding were considered as two-state process the GdnHCl-concentration at transition midpoint would have been 2.06 M which is higher than 1.55 M, and the dependence of ΔG on GdnHCl concentrations would have been as inset in Figure 17. Indeed the binding of Cu(II) makes the transition midpoint of apoCopC from 1.55 M shift to 2.06 M and stabilize the protein. However, there are evidently two slopes in dependence of ΔG on GdnHCl concentrations (Inset of Figure 17). This indicates that the equilibrium-unfolding reaction is three-state process, involving an intermediate species populated at 1.4 to 1.7 M guanidine hydrochloride [7].

| Protein | Denaturant | | -m kJ/M/mole | $[D]_{1/2}$ M | $\Delta G^0(\text{H}_2\text{O})/n$ kJ/mole | |
|--|------------|-------------------------------|-------------------------------|--|--|---|
| apoCopC | GdnHCl | | 16.16±0.22 | 1.55 | 24.98±0.31 | |
| | Urea | | 4.32±0.18 | 5.61 | 24.24±1.04 | |
| CopC-Ag ⁺ | GdnHCl | | 15.74±0.27 | 1.55 | 24.33±0.41 | |
| | | -m _{FI} kJ/M/mole | -m _{IU} kJ/M/mole | $\Delta G_{FI}^0(\text{H}_2\text{O})$ kJ/mole | $\Delta G_{IU}^0(\text{H}_2\text{O})$ kJ/mole | $\Delta G_{total}^0(\text{H}_2\text{O})/n$ kJ/mole |
| Cu ²⁺ -CopC | | 8.83±0.31 | 19.86±0.18 | 12.83±0.31 | 42.52±0.30 | 36.82 |
| Cu ²⁺ -CopC-Ag ⁺ | | 7.67±0.25 | 18.930±0.23 | 10.54±0.28 | 45.08±0.43 | 36.71 |
| Cu ²⁺ -Y79W-W83F | | 9.78±0.36 | 21.27±0.31 | 12.33±0.39 | 44.22±0.66 | 37.80 |
| | | | Urea - induced | | | |
| Cu ²⁺ -CopC | | 2.21±0.03 | 4.35±0.07 | 9.71±0.13 | 36.70±0.54 | 29.36 |

Table 2. Thermodynamic parameters for various forms of CopC from chemical denaturant-induced unfolding at pH 7.4, 25°C

According to the new model the structural element(s) of apoCopC is changed by the binding of Cu(II), from one-kind structural element(s) changing to two-kind structural elements, which one is more stable than another. Naturally the equilibrium-unfolding reaction of the protein displays three-state behavior. The data (●) measured guanidine hydrochloride experiment with Cu²⁺-CopC are fitted well in eq (19).

$$Y_{app} = 0.19 \times Y_{app}^1 (m_1, [D]_{1/2}^1) + 0.81 \times Y_{app}^2 (m_2, [D]_{1/2}^2) \quad (19)$$

where Y_{app}^1 and Y_{app}^2 are the unfolding transitions, $m_1, [D]_{1/2}^1$ and $m_2, [D]_{1/2}^2$ are the parameters described the stabilities of structural elements 1 and 2, respectively. A least-squares curve fitting analysis is used to calculate the $\Delta G_1^0(\text{H}_2\text{O})$, $\Delta G_2^0(\text{H}_2\text{O})$, m_1 , and m_2 . The $\Delta G_1^0(\text{H}_2\text{O})$ and $\Delta G_2^0(\text{H}_2\text{O})$ correspond to $\Delta G_{FI}^0(\text{H}_2\text{O})$ and $\Delta G_{IU}^0(\text{H}_2\text{O})$, and m_1 and m_2 are m_{FI} and m_{IU} respectively, in Table 2. From eqs (8) and (20) free energy change of Cu^{2+} -CopC can be calculated to be 36.82 kJ/mole.

$$\frac{\Delta G_{total}^0(\text{H}_2\text{O})}{n} = 0.19 \times \Delta G_1^0(\text{H}_2\text{O})(m_1, [D]_{1/2}^1) + 0.81 \times \Delta G_2^0(\text{H}_2\text{O})(m_2, [D]_{1/2}^2) \quad (20)$$

$$= 0.19 \times 12.83 + 0.81 \times 42.52 = 36.82$$

Cu^{2+} -CopC is consisted of two-kind structural elements. Thus the unfolding profile appears to involve two sequential transitions. The first transition corresponds to the unfolding of structural element one, whose free energy change is 12.83 kJ/mole and the guanidine hydrochloride concentration at the transition midpoint is 1.53 M, close to 1.55 M of apoCopC or apoCopC- Ag^+ . The second transition corresponds to the unfolding of another, whose free energy change is 42.52 kJ/mole and the guanidine hydrochloride concentration at the transition midpoint is 2.12 M. The probability of one appeared in the protein is 0.19 and another is 0.81. This indicates that the binding of $\text{Cu}(\text{II})$ makes the secondary structure of 81% integrative apo-CopC be stabilized. The stabilized energy $\Delta\Delta G_{\text{Cu}(\text{II})}^0$ is 11.84 kJ/mole. Since $\text{Cu}(\text{II})$ binds at N-terminal of apoCopC the first transition corresponds to the partial unfolding of apoCopC and it is the part the C-terminal of apoCopC.

Using urea as chemical denaturant the unfolding of Cu^{2+} -CopC shows three-state process. The free energy change is calculated to be 29.16 kJ/mole by using the new model. The stabilized energy $\Delta\Delta G_{\text{Cu}(\text{II})}^0$ is only 4.18 kJ/mole. At pH 7.4 apoCopC is a protein charged positively since the pI of the protein is 8.27. After binding of $\text{Cu}(\text{II})$ the positive charges of the protein is increased and anion ions would make Cu^{2+} -CopC be stable. As an ionic denaturant, guanidine hydrochloride makes Cu^{2+} -CopC be stable.

In a similar way the unfolding of Cu^{2+} -CopC- Ag^+ is studied by measuring the fluorescence ratio at 320 nm and 400 nm. Two transitions appear in the unfolding profile (Figure 17). Corresponding to the unfolding of C-terminal the first transition midpoint is shifted from 1.53 M to lower guanidine hydrochloride concentration (1.42 M), while the second transition midpoint is shifted from 2.12 M to higher guanidine hydrochloride concentration (2.38 M). Comparing with Cu^{2+} -CopC the binding of $\text{Ag}(\text{I})$ makes structural element one be unstable and structural element two be stable. This means that the structural element one and two are affected by the binding of $\text{Ag}(\text{I})$. Although the structural elements are marked as structural element one and two in Cu^{2+} -CopC- Ag^+ , they are different with that in Cu^{2+} -CopC.

The data (■) of Cu^{2+} -CopC- Ag^+ are fitted well in eq (21).

$$Y_{app} = 0.24 \times Y_{app}^1(m_1, [D]_{1/2}^1) + 0.76 \times Y_{app}^2(m_2, [D]_{1/2}^2) \quad (21)$$

It is noticed that Y_{app}^1 and Y_{app}^2 in eq (21) are different with that in eq (19). From eqs (8) free energy change of Cu^{2+} -CopC- Ag^+ can be calculated to be 36.71 kJ/mole. As $\text{Ag}(\text{I})$ binding to apoCopC the binding of $\text{Ag}(\text{I})$ to Cu^{2+} -CopC doesn't change free energy change of the protein and affected only the structural elements and the probabilities of structural elements appeared in the protein. Comparing eq (21) with eq (19), the contribution of structural element one is increased and two is decreased.

Hydrogen bonding and hydrophobic forces have major influence to the structure of native protein. Some molecules are often used in researching stability of native proteins since their perturbation on the hydrogen bonding and hydrophobic forces [31, 32]. Apo-Y79W-W83F is a mutant of apoCopC, in which tyrosine residue 79 is mutated as tryptophan and tryptophan residue is did as phenylalanine. As shown in Figure 18A the fluorescence spectrum of apoY79W-W83F is dominated by tryptophan residue at position 79 and centered at 328 nm. Comparing the fluorescence spectrum of apoCopC the maximum peak is shifted toward to red around 8 nm and the tryptophan residue is yet a typical for buried tryptophyl side chains in apolar environment. The protein binds one equivalent of Cu(II) with high affinity and the fluorescence at 328 nm is quenched[33].

Since the hydrogen bonding and hydrophobic forces in apoCopC are changed, the GdnHCl-induced unfolding profile of apo-Y79W-W83F shows an obvious two transitions. According to the new model apo-Y79W-W83F is consisted of two-kind structural elements, the unfolding curve can be fitted from Y_{app}^1 and Y_{app}^2 from eq (8), and free energy change can be calculated using eq (12). Although free energy change corresponding to apo-Y79W-W83F unfolding is nearly same with that of apoCopC (unpublished data) the structural elements in apo-Y79W-W83F are different with that of apoCopC.

Figure 18B shows GdnHCl-induced unfolding of Cu²⁺-Y79W-W83F (○). Analyzing the unfolding data according to two-state unfolding model, the free energy changes plotted as a function of denaturant concentration are an obviously inflection point, suggesting that GdnHCl-induced unfolding of Cu²⁺-Y79W-W83F does not proceed via a simple two-state process but involves one intermediate state. Using eq (8) the unfolding data of Cu²⁺-Y79W-W83F in Figure 18B can be fitted well. Y_{app}^1 and Y_{app}^2 are the unfolding curves of structural elements 1 and 2, respectively. The obtained thermodynamic parameters are listed Table 2.

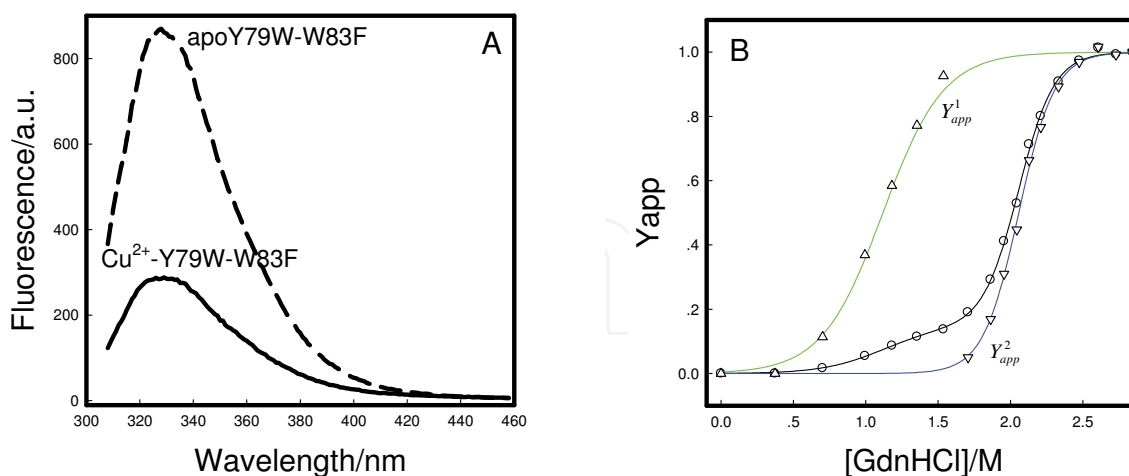


Fig. 18. Fluorescence spectra of Y79W-W83F (A) and GdnHCl-induced unfolding of Cu²⁺-Y79W-W83F by monitoring the fluorescence 400/320 nm ratio (○) (B). Lines are the fitting from two-state and three-state eqs. (Δ) and (∇) are the normalized data for first and second transitions, respectively.

Tryptophan residue 83 locates at N-terminal and tyrosine residue 79 locates at C-terminal of apoCopC. After binding Cu(II) the positions of the residues have no large change (Figure

15). Two transitions are observed in GdnHCl-induced unfolding profiles of Cu²⁺-CopC-Ag⁺, Cu²⁺-CopC, and Cu²⁺-Y79W-W83F. The first transition corresponds to the unfolding of C-terminal and second does to that of N-terminal. It can be seen that the mutation from tryptophan to phenylalanine residue at position of 83 makes the N-terminal stability be increased, while the mutation from tyrosine to tryptophan residue makes the C-terminal stability be decreased a little. This indicates that the aromatic ring stacking at position 83 plays an important role in keeping the secondary native structure of apoCopC.

7. Summary

A new model to calculate the free energy change of proteins unfolding is presented. In the new proposed model proteins are consisted of different structural elements; the unfolding of structural element obeys two-state mechanism and the free energy change of the element can be obtained by using linear extrapolation method; if the protein is consisted of same structural elements unfolding of the protein displays a two-state process, while the unfolding of the protein shows a multi-state behavior; A least-square fitting is used to analyze the contribution of structural element to the protein and free energy change of the protein is the probable summing of all structural element. The model can be used to analyze and compare the stability of proteins, which are similar in size and structure.

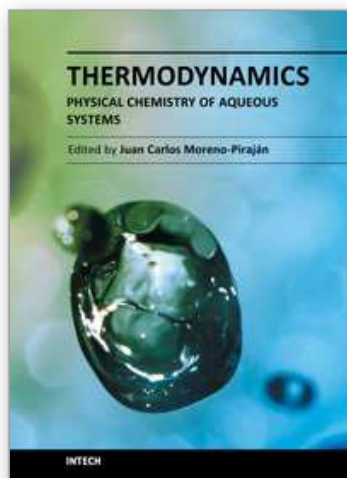
8. References

- [1] Santoro M M and Bolen D W, A test of the linear extrapolation of unfolding free energy changes over an extended denaturant concentration range, *Biochemistry*, 1992, 31, 4901-4907.
- [2] Bolen D W and Santoro M M, Unfolding free energy changes determined by the linear extrapolation method. 2. Incorporation of ΔG_{0N-U} values in a thermodynamic cycle, *Biochemistry*, 1988, 27, 8069-8074.
- [3] Santoro M M and Bolen D W, Unfolding free energy changes determined by the linear extrapolation method. 1. Unfolding of phenylmethanesulfonyl α -chymotrypsin using different denaturant, *Biochemistry*, 1988, 27, 8063-8068.
- [4] Matthews C R and Crisanti M M, Urea-induced unfolding of the α subunit of tryptophan synthase: evidence for a multistate process, *Biochemistry*, 1981, 20, 784-792.
- [5] Muzammil S, Kumar Y and Tayyab S, Anion-induced stabilization of human serum albumin prevents the formation of intermediate during urea denaturation, *Proteins: Structure, Function, and Genetics*, 2000, 40, 29-38.
- [6] Xu X L, Liu Q L, Yu H M and Xie Y S, Ca(II)- and Tb(III)-induced stabilization and refolding of anticoagulation factor I from the venom of *Agkistrodon acutus*, *Protein Science*, 2002, 11, 944-956.
- [7] Hussain F, Sedlak E and Wittung-Stafshede P, Role of copper in folding and stability of cupredoxin-like copper-carrier protein CopC, *Arch Biochem Biophys*, 2007, 467, 58-66.
- [8] Wang X Y, Zhang Z R and Perrett S, Characterization of the activity and folding of the glutathione transferase from *Escherichia coli* and the roles of residues Cys10 and His106, *Biochem J*, 2009, 417, 55-64.
- [9] Englander S W, Protein folding intermediates and pathways studied by hydrogen exchange. *Annu Rev Biophys Biomol Struct*, 2000, 29, 213-239.

- [10] Soderberg B O, Three-dimensional structure of Escherichia coli thioredoxin-S2 to 2.8 Å resolution. *Proc Natl Acad Sci USA*, 1975, 72, 2305-2309.
- [11] Katti S K, LeMaster D M, Crystal structure of thioredoxin from Escherichia coli at 1.68Å resolution. *J Mol Biol*, 1990, 212, 167-184.
- [12] Voet D, Voet J G, *Biochemistry*, Chapter 7: Three-dimensional structures of proteins, Second Ed. 1995, p141.
- [13] Greene Jr R F, Pace C N, Urea and guanidine hydrochloride denaturation of ribonuclease, lysozyme, α -chymotrypsin, and β -lactoglobulin. *J Biol Chem*, 1974, 249, 5388-5393.
- [14] Wallevik K, Reversible denaturation of human serum albumin by pH, Temperature, and Guanidine Hydrochloride Followed by Optical Rotation. *J Biol Chem*, 1973, 248, 2650-2655.
- [15] Kumar Y, Muzammil S, and Tayyab S, Influence of Fluoro, Chloro and Alkyl Alcohols on the Folding Pathway of Human Serum Albumin, *J Biochem*, 2005, 138, 335-341.
- [16] Halim A A A, Kadir H A, and Tayyab S, Bromophenol blue binding as a probe to study urea and guanidine hydrochloride denaturation of bovine serum albumin. *J Biochem*. 2008, 144, 33-38.
- [17] Mostafa R T, Moghaddamnia S H, Ranjbar B, Amani M, Marashi S A, Conformational study of human serum albumin in pre-denaturation temperatures by differential scanning calorimetry, circular dichroism and UV spectroscopy. *J Biochem Mol Biol*, 2006, 39, 530-536.
- [18] Yang B S, Yang P, Song L H, The binding of Gd(III) to human serum albumin, *Kexue Tongbao*, 1984, 29, 1502-1505.
- [19] Yang B S, Yang P, The action of rare earth ions with human serum albumin. *Chin J Biochem Biophys*, 1989, 21, 302-305.
- [20] Ong H N, Arumugam B, Tayyab S, Succinylation-induced conformational destabilization of lysozyme as studied by guanidine hydrochloride denaturation. *J Biochem*, 2009, 146, 895-904.
- [21] Arnesano F, Banci L, Bertini I, et al. Solution structure of CopC: a cupredoxin-like protein involved in copper homeostasis. *Structure*, 2002, 10, 1337-1347.
- [22] Arnesano F, Banci L, Bertini I, et al. A strategy for the NMR characterization of type II copper(II) proteins: the case of the copper trafficking protein CopC from *Pseudomonas syringae*. *J Am Chem Soc*, 2003, 125, 7200-7208.
- [23] Koay M, Zhang L Y, Yang B S, Maher M J, Xiao Z G, Wedd A G, CopC Protein from *Pseudomonas syringae*: Intermolecular Transfer of Copper from Both the Copper(I) and Copper(II) Sites. *Inorg Chem*, 2005, 44, 5203-5205.
- [24] Pang E G, Zhao Y Q, Yang B S, Fluorescence study on the interaction between apoCopC and cupric. *Chin Sci Bullet*, 2005, 50, 2302-2305.
- [25] Zheng X Y, Pang E G, Zhao Y Q, Yang B S. Spectral studies on the interaction between mercuric ion and apoCopC. *Chin J Chem*, 2007, 25: 630-634.
- [26] Song Z, Zheng X Y, Pang E G, Yang B S, Spectral studies on the interaction of Vitamin B6 with different CopC. *Chem J Chin Univ*, 2011, 32 .
- [27] Zheng X Y, Pang E G, Zhao Y Q, Jiao Y, Yang B S, Investigation on the Inclusion Behavior of ApoCopC with Vitamin B6. *Supramol Chem*, 2008, 20, 553-557.
- [28] Li H Q, Zheng X Y, Pang E G, Zhao Y Q, Yang B S, The effect of Trp83 mutant on the properties of CopC. *Spectrochim Acta A*, 2008, 70(2) , 384-388.

- [29] Zheng X Y, Pang E G, Li H Q, Zhao Y Q, Yang B S, The role of cupric in maintaining the structure of CopC. *Chin Sci Bullet* · 2007, 52, 743-747.
- [30] Li H Q, Zhao Y Q, Yang B S, Apo-CopC and CopC-Cu(II) unfolding characteristics in GuHCl solution. *Chin J Chem*, 2009, 27, 1762-1766.
- [31] Li H Q, Zhao Y Q, Zheng X Y, Yang B S · Fluorescence spectra study the perturbations of CopC native fold by 2-p-toluidinynaphthalene-6-sulfonate. *Spectrochim Acta A*, 2009, 72(1), 56-60.
- [32] Li H Q, Zheng X Y, Zhao Y Q, Yang B S, Conformation disturbance of CopC by α -naphthylamine. *Chem Res Chin Univ*, 2009, 25(3), 269-272.
- [33] Zheng X Y, Yang B S, An improved method for measuring the stability of a three-state unfolding protein. *Chinese Sci Bullet*, 2010, 55, 4120-4124.

IntechOpen



Thermodynamics - Physical Chemistry of Aqueous Systems

Edited by Dr. Juan Carlos Moreno Piraján

ISBN 978-953-307-979-0

Hard cover, 434 pages

Publisher InTech

Published online 15, September, 2011

Published in print edition September, 2011

Thermodynamics is one of the most exciting branches of physical chemistry which has greatly contributed to the modern science. Being concentrated on a wide range of applications of thermodynamics, this book gathers a series of contributions by the finest scientists in the world, gathered in an orderly manner. It can be used in post-graduate courses for students and as a reference book, as it is written in a language pleasing to the reader. It can also serve as a reference material for researchers to whom the thermodynamics is one of the area of interest.

How to reference

In order to correctly reference this scholarly work, feel free to copy and paste the following:

Yang BinSheng (2011). The Stability of a Three-State Unfolding Protein, Thermodynamics - Physical Chemistry of Aqueous Systems, Dr. Juan Carlos Moreno Piraján (Ed.), ISBN: 978-953-307-979-0, InTech, Available from: <http://www.intechopen.com/books/thermodynamics-physical-chemistry-of-aqueous-systems/the-stability-of-a-three-state-unfolding-protein>

INTECH
open science | open minds

InTech Europe

University Campus STeP Ri
Slavka Krautzeka 83/A
51000 Rijeka, Croatia
Phone: +385 (51) 770 447
Fax: +385 (51) 686 166
www.intechopen.com

InTech China

Unit 405, Office Block, Hotel Equatorial Shanghai
No.65, Yan An Road (West), Shanghai, 200040, China
中国上海市延安西路65号上海国际贵都大饭店办公楼405单元
Phone: +86-21-62489820
Fax: +86-21-62489821

© 2011 The Author(s). Licensee IntechOpen. This chapter is distributed under the terms of the [Creative Commons Attribution-NonCommercial-ShareAlike-3.0 License](#), which permits use, distribution and reproduction for non-commercial purposes, provided the original is properly cited and derivative works building on this content are distributed under the same license.

IntechOpen

IntechOpen